Journal of Southeast University (English Edition) Vol. 39, No. 3, pp. 213 - 224 Sept. 2023 ISSN 1003—7985

Improved complex modal superposition method with inclusion of overdamped modes

Chen Yong[1, 2] Donald M. McFarland[3, 4] Billie F. Spencer, Jr.[2] Lawrence A. Bergman[3]

([1]College of Civil Engineering and Architecture, Zhejiang University, Hangzhou 310027, China)
([2]Department of Civil and Environmental Engineering, University of Illinois at Urbana-Champaign, Urbana 61801, USA)
([3]Department of Aerospace Engineering, University of Illinois at Urbana-Champaign, Urbana 61801, USA)
([4]College of Mechanical Engineering, Zhejiang University of Technology, Hangzhou 310014, China)

Abstract: To address the involvement of overdamped complex modes that appear in a nonproportionally damped system, an improved complex mode superposition (ICMS) theory is proposed for forced vibration analysis, which suggests the use of exact modes in pairs for CMS-based dynamic analysis of whether the modes are overdamped or not. A typical nonproportionally damped system, namely, a cantilever beam with attached multiple arbitrarily placed external dampers, is considered an example because the first mode of the system is likely to be overdamped with the increase in damping. First, the relationship between the response in a complex modal space and the actual dynamic response is elucidated, based on which complete theoretical ICMS approaches for attaining time-domain response, transfer functions, and variances are expounded in detail. By decomposing the governing equation into real and imaginary parts, the original equation of motion in the complex domain is represented by an augmented state-space equation with real-valued matrices, which considerably reduces the difficulties observed in computing the time-varying response using complex-valued matrices. Additionally, for external excitations that can be regarded as filtered white noise, an efficient method for evaluating the variance response is proposed, which effectively reduces the computational cost. The results from the application of the proposed CMS-based methods are compared with those obtained by an assumed-mode (AM) method and finite element analysis (FEA). It can be found that the current results are closer to those obtained by FEA than those by the AM method. Finally, the optimal damping and optimal position of the dampers are investigated using an enumeration method, which reveals that the use of multiple dampers with small damping demonstrates a better effect than that of a single damper with large damping.

Key words: nonclassically damped system; continuous system; forced vibration; complex mode superposition method; overdamped mode; dynamic response

DOI: 10.3969/j.issn.1003 - 7985.2023.03.001

Received 2023-03-02, **Revised** 2023-05-22.

Biographies: Chen Yong (1974—), male, Ph. D., professor; Donald M. McFarland (corresponding author), male, doctor, professor, dmmcf@dmmcf.net.

Foundation items: National Science Foundation through TeraGrid Resources provided by the National Center for Supercomputing Applications (No. TG-MSS100016).

Citation: Chen Yong, Donald M. McFarland, Billie F. Spencer, Jr., et al. Improved complex modal superposition method with inclusion of overdamped modes[J]. Journal of Southeast University (English Edition), 2023, 39(3): 213 - 224. DOI: 10.3969/j.issn.1003 - 7985.2023.03.001.

In the analysis of structures that exhibit natural modes of vibration, the presence of discrete energy-dissipation devices is recognized to disturb the mode shapes of the original system[1] and consequently leads to a nonclassically damped system (NCDS) if the Caughey-O'Kelly condition[2-3] is not fulfilled. Even today, the mode-superposition method remains attractive in performing a forced vibration analysis[4] owing to its remarkable qualities, such as conceptual simplicity and capability to reduce the order of a system by treating the vibration of the system as a linear combination of finite modal vibrations. The modal methods for NCDSs mainly fall into two categories: 1) Assumed-mode (AM) methods[4-14] in which approximate admissible shape functions, usually the mode shapes of the undisturbed system, are adopted; 2) Complex mode superposition (CMS) methods[15-24], which conventionally utilize the exact modes formed in a complex domain. The CMS method appears to be more promising because the complex eigenvalues and eigenfunctions, which yield a modal vibration with varying configuration rather than a constant configuration found in classically damped systems, are more suitable for characterizing the complicated dynamic behavior of NCDS[15].

Earlier studies on the use of complex modes mainly focused on discrete structures. One can be traced back to Foss[16], who proposed a theoretical approach where a structural motion could be expanded into a modal series, and the nonhomogeneous solutions of the dynamic system could thus be achieved. With regard to a nonclassically damped multi-degree-of-freedom (DOF) system, Veletsos and Ventura[15] elaborated on the application of the CMS method to free and forced vibration analyses in which a shear-beam-type three-story structure was introduced as an example. Recently, Zhao and Zhang[17] have proposed an acceleration technique where the CMS method that used truncated complex modes could be compensated. de Domenico and Ricciardi[18] introduced two real-valued measures to determine the number of complex modes to retain in a reduced-order model.

Although extensive studies related to the application of the CMS method to discrete structures have been conducted, the applicability of CMS for a continuous system remains limited, and only a few relevant studies can be

found in the literature due to the lack of exact complex modes and corresponding natural frequencies of NCDS[19]. Oliveto and Santini[20] derived the complex modes of a soil-structure system, which was simplified as two connected shear beams, and applied the CMS method to its dynamic analysis. Oliveto et al.[19] then extended the study to a simply supported Bernoulli-Euler beam with two rotational viscous dampers that were individually attached at the beam ends and investigated the dynamic behavior of the system undergoing free and forced vibration. By considering a Bernoulli-Euler beam with viscoelastic boundary supports at its ends, Fan et al.[21] demonstrated the complex modes of the system using complex stiffness coefficients, and the CMS method, in association with the derived complex modes, was then applied to obtain the dynamic response induced by harmonic excitations. By introducing an independent representation of the momentum for damped continuous systems, Krenk[22] formulated a general motion equation in a state-space form in which both the stiffness and damping operators were self-adjoint and symmetric. He considered a cable with a lateral viscous damper and a beam with two identical rotational viscous dampers attached at its ends for their case studies. For a pinned-pinned cable attached to rotational dampers and springs at their ends, Impollonia et al.[23] performed a CMS method-based time-domain dynamic analysis by splitting the modal decoupled equation of motion into real and imaginary parts. For the axial vibration of a rod with various arbitrarily placed viscous damping devices such as external (grounded), mass, and internal spring dampers, Alati et al.[24] demonstrated the exact closed-form eigenfunctions and characteristic equations and revealed that the CMS method, compared with the AM method, inherently satisfied the discontinuity conditions at the locations of the damping devices. Nevertheless, for the incorporation of overdamped modes, relevant development of the CMS method was not well elucidated in previous studies. The exact modes are commonly assumed to be complex conjugates; however, this is not true when overdamped modes are involved[25].

The current study presents theoretical approaches for forced vibration analysis in both the frequency and time domains using a multi-damper-beam system whose first mode is prone to overdamping with the increase in external damping[25]. An improved CMS (ICMS) theory is proposed in the present study, in which the exact modes should be strictly used in pairs to decouple the vibration response, whether the modes are overdamped or not. A pair of overdamped modes consist of the modes that correspond to two real-valued solutions of the same characteristic equation. Consequently, pairwise exact modes must be adopted in converting the results in a complex modal space into actual vibration responses. For the convenience of the forced vibration analysis, the relevant methodologies presented herein are formulated in a state space. Moreover, the original continuous system is transformed into a reduced-order system by considering the presence of overdamped modes. For time-domain analysis, an augmented motion equation is proposed in which all of the matrices are real-valued, where the real and imaginary parts of the modal vibrations can be simultaneously obtained. For frequency-domain analysis, the transfer functions are found using Laplace transformation in association with modal decoupling techniques. An estimation equation for variance response is presented in terms of the variance response of a modal vibration. The modal variance response can be approximated by solving a Lyapunov equation in the modal space. The results are corroborated by finite element analyses (FEAs). Finally, we consider the random excitation by white noise located at the midspan. The optimal damping and optimal location are identified for two objective measures, namely, variance in dynamic response at the free end and spatial average variance. The formulas presented herein are nondimensionalized, which enables the identification of minimal sets of parameters that govern the inherent dynamic characteristics and facilitate the comparison of similar systems.

1 Problem Formulation

For forced vibration analysis, we consider a general damper-beam system, namely, a cantilevered beam with multiple arbitrarily placed external dampers. The exact complex modes of this system were presented in a previous study[25], and the transfer functions and variance responses of a single-damper-attached beam were investigated by constructing a closed-loop system in the frequency domain[26-27]. Fig. 1 shows that a Cartesian coordinate system is employed to describe the beam vibration, and the origin is set at the clamped end of the beam. Thus, the x coordinate is along the beam, and y denotes the displacement of the beam undergoing vibration. The bending stiffness of the beam is characterized by EI, where E is Young's modulus and I is the cross-sectional second moment of the area around the neutral axis. The length of the beam is l, and m denotes the mass per unit length. The number of viscous dampers is J, and the damping coefficient of the i-th damper is denoted as C_i^{d}. The distance

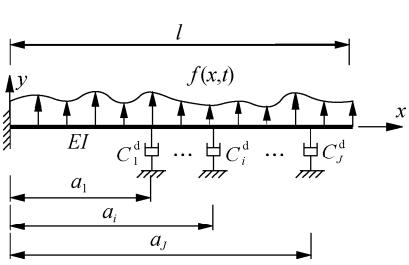

Fig. 1 Cantilever beam with dampers and subjected to external excitation

from the i-th damper to the clamped end of the beam is denoted by a_i. We note that the installed dampers are sequentially numbered, i.e., $0 \leqslant a_1 \leqslant a_2 \leqslant \ldots \leqslant a_J \leqslant l$. The distributed time-varying loading on the beam is $f(x, t)$, where t is the time. The beam is modeled as a Bernoulli-Euler beam without internal damping.

By using d'Alembert's principle, the governing equation of this system can be expressed as

$$EI\frac{\partial^4 y(x,t)}{\partial x^4} + \sum_{i=1}^{J} C_i^{\mathrm{d}}\frac{\partial y(x,t)}{\partial t}\delta(x-a_i) + m\frac{\partial^2 y(x,t)}{\partial t^2} = f(x,t) \tag{1a}$$

$$Y(0)=0,\ \frac{\mathrm{d}}{\mathrm{d}x}Y(0)=0,\ \frac{\mathrm{d}^2}{\mathrm{d}x^2}Y(l)=0,\ \frac{\mathrm{d}^3}{\mathrm{d}x^3}Y(l)=0 \tag{1b}$$

where $\delta(\ )$ is the Dirac delta function, and Eq. (1b) accounts for the boundary conditions. Without loss of generality, Eq. (1) can be nondimensionalized by

$$\tilde{y}=y/l,\ \tilde{x}=x/l,\ \alpha_i=a_i/l,\ \tilde{t}=t\omega_0$$
$$\omega_0=\sqrt{\frac{EI}{ml^4}},\ c_i=C_i^{\mathrm{d}}\frac{\omega_0 l^3}{EI}=\frac{C_i^{\mathrm{d}}l}{\sqrt{mEI}} \tag{2}$$

Thus, we obtain

$$\frac{\partial^4\tilde{y}(\tilde{x},\tilde{t})}{\partial\tilde{x}^4} + \sum_{i=1}^{J} c_i\frac{\partial\tilde{y}(\tilde{x},\tilde{t})}{\partial\tilde{t}}\delta(\tilde{x}-\alpha_i) + \frac{\partial\tilde{y}^2(\tilde{x},\tilde{t})}{\partial\tilde{t}^2} = \tilde{f}(\tilde{x},\tilde{t}) \tag{3a}$$

$$\tilde{Y}(0)=0,\ \frac{\mathrm{d}}{\mathrm{d}\tilde{x}}\tilde{Y}(0)=0,\ \frac{\mathrm{d}^2}{\mathrm{d}\tilde{x}^2}\tilde{Y}(1)=0,\ \frac{\mathrm{d}^3}{\mathrm{d}\tilde{x}^3}\tilde{Y}(1)=0 \tag{3b}$$

where

$$\tilde{f}(\tilde{x},\tilde{t}) = \frac{l^3}{EI}f(x,t),\ \text{or}\ ml^2\omega_0^2\int_0^1\tilde{f}(\tilde{x},\tilde{t})\,\mathrm{d}\tilde{x} = \int_0^l f(x,t)\,\mathrm{d}x \tag{4}$$

For free vibration, we obtain

$$\frac{\partial^4\tilde{y}(\tilde{x},\tilde{t})}{\partial\tilde{x}^4} + \sum_{i=1}^{J} c_i\frac{\partial\tilde{y}(\tilde{x},t)}{\partial\tilde{t}}\delta(\tilde{x}-\alpha_i) + \frac{\partial\tilde{y}^2(\tilde{x},\tilde{t})}{\partial\tilde{t}^2} = 0 \tag{5}$$

By using separation of variables, the solution of Eq. (5) has the following form[25]:

$$\tilde{y}(\tilde{x},\tilde{t}) = D_1\varphi(\omega,\tilde{x})\,\mathrm{e}^{\omega t} \tag{6a}$$

$$\omega = \mathrm{j}\lambda^2 \tag{6b}$$

$$\mathrm{j}=\sqrt{-1} \tag{6c}$$

where D_1 is an undetermined parameter in the complex domain, $\varphi(\omega,\tilde{x})$ is the complex mode shape, ω is the complex natural frequency, and λ is the wave number. Eq. (5) is solved by substituting Eq. (6) into Eq. (5) and using the argument principle method[25]. The corresponding wave numbers, natural frequencies, and mode shapes are derived in the complex domain. For details, interested readers may refer to Ref. [25]. Note that the natural frequencies and mode shapes are grouped in pairs[25]. Symbols ω and ω^* are utilized to represent a pair of natural frequencies, whereas symbols φ and φ^* represent a pair of natural modes.

Subscripts n and k denote the sequential number of the modes, natural frequencies, or wave numbers, which are sorted using pseudoundamped natural frequencies in ascending order. Thus, Eq. (6a) yields

$$\tilde{y}_n(\tilde{x},\tilde{t}) = D_1\varphi_n(\omega_n,\tilde{x})\,\mathrm{e}^{\omega_n t} \tag{7}$$

where $\tilde{y}_n(\tilde{x},\tilde{t})$ is the time-varying displacement response corresponding to the n-th natural frequency. Substituting Eq. (7) into Eq. (5) yields the following for the n-th mode:

$$\frac{\mathrm{d}^4\varphi_n}{\mathrm{d}\tilde{x}^4} + \sum_{i=1}^{J} c_i\omega_n\varphi_n\delta(\tilde{x}-\alpha_i) + \omega_n^2\varphi_n = 0 \tag{8}$$

In a similar manner, the k-th mode expression is obtained as

$$\frac{\mathrm{d}^4\varphi_k}{\mathrm{d}\tilde{x}^4} + \sum_{i=1}^{J} c_i\omega_k\varphi_k\delta(\tilde{x}-\alpha_i) + \omega_k^2\varphi_k = 0 \tag{9}$$

Subtracting the integration of Eq. (8) that is premultiplied by φ_k from the integration of Eq. (9) premultiplied by φ_n yields the following:

$$\int_0^1\{\varphi_k,\omega_k\varphi_k\}\begin{bmatrix}\sum_{i=1}^{J} c_i\delta(\tilde{x}-\alpha_i) & 1\\ 1 & 0\end{bmatrix}\begin{Bmatrix}\varphi_n\\ \omega_n\varphi_n\end{Bmatrix}\mathrm{d}\tilde{x} = 0 \qquad \omega_k \neq \omega_n \tag{10}$$

Similarly, subtracting the integration of Eq. (8) that is premultiplied by $\omega_k\varphi_k$ from the integration of Eq. (9) premultiplied by $\omega_n\varphi_n$ yields

$$\int_0^1\{\varphi_k,\omega_k\varphi_k\}\begin{bmatrix}\frac{\partial^4}{\partial x^4} & 0\\ 0 & -1\end{bmatrix}\begin{Bmatrix}\varphi_n\\ \omega_n\varphi_n\end{Bmatrix}\mathrm{d}\tilde{x} = 0 \qquad \omega_k \neq \omega_n \tag{11}$$

Eqs. (10) and (11) are the first and second orthogonality conditions, respectively.

2 Reduced-Order System with Finite DOFs

Discrete systems with motion equations in a matrix form, which are achieved by applying the CMS and AM methods, are presented in this section. Note that the original system has infinite DOFs. Both the CMS and AM methods are capable of producing a reduced-order system with finite DOFs using the truncated modes.

2.1 CMS method

The CMS method lets the vibration response of the system be expressed as a linear combination of modal vibrations with corresponding natural frequencies. Thus, the vibration of the system is approximately expressed as

$$\begin{Bmatrix} \tilde{y} \\ \dfrac{\partial \tilde{y}}{\partial \tilde{t}} \end{Bmatrix} \approx \sum_{i=1}^{N} \begin{Bmatrix} \varphi_i \\ \omega_i \varphi_i \end{Bmatrix} p_i(\tilde{t}) + \sum_{i=1}^{N} \begin{Bmatrix} \varphi_i^* \\ \omega_i^* \varphi_i^* \end{Bmatrix} p_i^*(\tilde{t}) \quad (12)$$

where $p_i(\tilde{t})$ and $p_i^*(\tilde{t})$ in Eq. (12) are the generalized coordinates of the i-th associated mode φ_i and its counterpart φ_i^*, respectively. For underdamped complex modes, φ_i^* denotes the conjugated complex mode of φ_i.

Let the following equations be true:

$$\boldsymbol{\psi} = \{\psi_1, \psi_2, \ldots, \psi_n, \ldots, \psi_{2N}\} = \{\varphi_1, \varphi_2, \ldots, \varphi_i, \ldots, \varphi_N, \varphi_1^*, \ldots, \varphi_i^*, \ldots, \varphi_N^*\} \quad (13a)$$

$$\boldsymbol{q} = \{q_1(\tilde{t}), q_2(\tilde{t}), \ldots, q_n(\tilde{t}), \ldots, q_{2N}(\tilde{t})\}^{\mathrm{T}} = \{p_1(\tilde{t}), p_2(\tilde{t}), \ldots, p_i(\tilde{t}), \ldots, p_N(\tilde{t}), p_1^*(\tilde{t}), \ldots, p_i^*(\tilde{t}), \ldots, p_N^*(\tilde{t})\}^{\mathrm{T}} \quad (13b)$$

$$\boldsymbol{\Lambda} = \{\Lambda_1, \Lambda_2, \ldots, \Lambda_n, \ldots, \Lambda_{2N}\} = \{\omega_1, \omega_2, \ldots, \omega_i, \ldots, \omega_N, \omega_1^*, \omega_2^*, \ldots, \omega_i^*, \ldots, \omega_N^*\} \quad (13c)$$

where $\boldsymbol{\psi}$, $\boldsymbol{q}$, and $\boldsymbol{\Lambda}$ are the modal, generalized coordinate, and frequency vectors, respectively. Thus, Eq. (12) can be rewritten as

$$\begin{Bmatrix} \tilde{y} \\ \dfrac{\partial \tilde{y}}{\partial \tilde{t}} \end{Bmatrix} \approx \sum_{n=1}^{2N} \begin{Bmatrix} \psi_n \\ \Lambda_n \psi_n \end{Bmatrix} q_n(\tilde{t}) = \begin{bmatrix} \boldsymbol{\psi} \\ \boldsymbol{\Lambda} \circ \boldsymbol{\psi} \end{bmatrix} \boldsymbol{q} \quad (14)$$

where notation "$\circ$" is the Hadamard product operator. The displacement response can be computed using

$$\tilde{y} \approx \boldsymbol{\psi} \boldsymbol{q} \quad (15)$$

The motion equation represented by Eq. (3) is thus re-expressed in the state space as

$$\begin{bmatrix} \dfrac{\partial^4}{\partial \tilde{x}^4} & 0 \\ 0 & -1 \end{bmatrix} \begin{Bmatrix} \tilde{y} \\ \dfrac{\partial \tilde{y}}{\partial \tilde{t}} \end{Bmatrix} + \begin{bmatrix} \sum_{i=1}^{J} c_i \delta(\tilde{x} - \alpha_i) & 1 \\ 1 & 0 \end{bmatrix} \frac{\partial}{\partial \tilde{t}} \begin{Bmatrix} \tilde{y} \\ \dfrac{\partial \tilde{y}}{\partial \tilde{t}} \end{Bmatrix} = \begin{Bmatrix} \tilde{f} \\ 0 \end{Bmatrix} \quad (16)$$

The operators in the coefficient matrices are found to be self-adjoint. Thus, Eq. (16) can be diagonalized by its eigenfunctions.

Substituting Eq. (14) into Eq. (16) and integrating Eq. (16), which is premultiplied by $\{\psi_k, \Lambda_k \psi_k\}$, yield the following:

$$\sum_{n=1}^{2N} q_n \int_0^1 \{\psi_k, \Lambda_k \psi_k\} \begin{bmatrix} \dfrac{\partial^4}{\partial x^4} & 0 \\ 0 & -1 \end{bmatrix} \begin{Bmatrix} \psi_n \\ \Lambda_n \psi_n \end{Bmatrix} \mathrm{d}\tilde{x} + \sum_{n=1}^{2N} \frac{\partial q_n}{\partial \tilde{t}} \int_0^1 \{\psi_k, \Lambda_k \psi_k\} \begin{bmatrix} \sum_{i=1}^{J} c_i \delta(\tilde{x} - \alpha_i) & 1 \\ 1 & 0 \end{bmatrix} \begin{Bmatrix} \psi_n \\ \Lambda_n \psi_n \end{Bmatrix} \mathrm{d}\tilde{x} = \int_0^1 \{\psi_k, \Lambda_k \psi_k\} \begin{Bmatrix} \tilde{f} \\ 0 \end{Bmatrix} \mathrm{d}\tilde{x} \quad (17)$$

Then, by applying the orthogonality conditions given in Eqs. (10) and (11), we have

$$q_k \left\{ \int_0^1 \psi_k \frac{\partial^4 \psi_k}{\partial x^4} \mathrm{d}\tilde{x} - \Lambda_k^2 \int_0^1 \psi_k^2 \mathrm{d}\tilde{x} \right\} + \frac{\partial q_k}{\partial \tilde{t}} \left\{ \int_0^1 \sum_{i=1}^{J} c_i \delta(\tilde{x} - \alpha_i) \psi_k^2 \mathrm{d}\tilde{x} + 2\Lambda_k \int_0^1 \psi_k^2 \mathrm{d}\tilde{x} \right\} = \int_0^1 \psi_k \tilde{f} \mathrm{d}\tilde{x} \quad (18)$$

We note that

$$\int_0^1 \psi_k \frac{\partial^4 \psi_k}{\partial x^4} \mathrm{d}\tilde{x} - \Lambda_k^2 \int_0^1 \psi_k^2 \mathrm{d}\tilde{x} = -\Lambda_k \left\{ \int_0^1 \sum_{i=1}^{J} c_i \delta(\tilde{x} - \alpha_i) \psi_k^2 \mathrm{d}\tilde{x} + 2\Lambda_k \int_0^1 \psi_k^2 \mathrm{d}\tilde{x} \right\} \quad (19)$$

Eq. (18) yields

$$\frac{\partial q_k}{\partial \tilde{t}} = \Lambda_k q_k + \frac{\int_0^1 \psi_k \tilde{f} \mathrm{d}\tilde{x}}{\sum_{i=1}^{J} c_i \psi_k(\alpha_i)^2 + 2\Lambda_k \int_0^1 \psi_k^2 \mathrm{d}\tilde{x}} \quad (20)$$

As Eq. (20) holds for all $k = 1, 2, \ldots, 2N$,

$$\frac{\mathrm{d}}{\mathrm{d}\tilde{t}} \boldsymbol{q} = \boldsymbol{\Omega} \boldsymbol{q} + \boldsymbol{B} \boldsymbol{u} \quad (21)$$

where

$$\boldsymbol{\Omega} = \mathrm{diag}(\Lambda_k) \qquad k = 1, 2, \ldots, 2N \quad (22)$$

$$\boldsymbol{B} = \mathrm{diag}(B_k) \qquad k = 1, 2, \ldots, 2N$$

$$B_k = \frac{1}{\sum_{i=1}^{J} c_i \psi_k(\alpha_i)^2 + 2\Lambda_k \int_0^1 \psi_k \psi_k \mathrm{d}\tilde{x}} \quad (23)$$

$$\boldsymbol{u} = \{u_1, u_2, \ldots, u_k, \ldots, u_{2N}\}^{\mathrm{T}}, \quad u_k = \int_0^1 \psi_k \tilde{f} \mathrm{d}\tilde{x} \quad (24)$$

where $\boldsymbol{\Omega}$ and $\boldsymbol{B}$ are the state and input matrices of the system in a complex modal space, respectively; $\boldsymbol{u}$ is the input vector of the system in a complex modal space.

Eq. (21) represents a governing motion equation in a complex modal space and states that the original system can be decoupled. Then, the dynamic response governed by Eq. (3) can be approximated by solving Eq. (21).

We need to note that the response must be computed using Eq. (15) instead of the following:

$$\tilde{y}(\tilde{x}, \tilde{t}) = 2\mathrm{Re}\left(\sum_{n=1}^{N} \varphi_n(\tilde{x}) p_n(\tilde{t}) \right) \quad (25)$$

which is frequently used in accordance with the assumption that the natural frequencies and modes are in conju-

gate pairs[20]. This assumption does not hold for every NCDS because, in some cases, overdamped modes with low natural frequency will appear.

2.2 AM method

The orthogonality conditions for the modes of a cantilever beam with no attached damper (the undamped/undisturbed system) are expressed as

$$\int_0^1 \widehat{\varphi}_n(\tilde{x})\,\widehat{\varphi}_k(\tilde{x})\,\mathrm{d}\tilde{x} = 0 \qquad n \neq k \tag{26a}$$

$$\int_0^1 \widehat{\varphi}_n''(\tilde{x})\,\widehat{\varphi}_k''(\tilde{x})\,\mathrm{d}\tilde{x} = 0 \qquad n \neq k \tag{26b}$$

$$\int_0^1 \widehat{\varphi}_n''(\tilde{x})\,\widehat{\varphi}_n''(\tilde{x})\,\mathrm{d}\tilde{x} = \widehat{\omega}_n^2 \int_0^1 \widehat{\varphi}_n(\tilde{x})\,\widehat{\varphi}_n(\tilde{x})\,\mathrm{d}\tilde{x} \neq 0 \tag{26c}$$

where $\widehat{\omega}_n$ is the n-th natural frequency of the undamped system; $\widehat{\varphi}_n$ is the n-th mode of the undamped system; symbol " $\widehat{\ }$ " in the variable denotes that the variable is for the AM method.

The vibration of a beam may be approximated using a truncated series of N modes as follows:

$$\tilde{y}(\tilde{x},\tilde{t}) \approx \sum_{n=1}^{N} \widehat{\varphi}_n(\tilde{x})\,\widehat{q}_n(\tilde{t}) = \widehat{\boldsymbol{\varphi}}\widehat{\boldsymbol{q}} \tag{27}$$

where $\widehat{q}_n(\tilde{t})$ is the n-th generalized coordinate; $\widehat{\boldsymbol{\varphi}}$ is the AM-method-based modal matrix that comprises N undamped modes; $\widehat{\boldsymbol{q}}$ is the generalized coordinate vector of the AM method. They can be expressed as

$$\widehat{\boldsymbol{q}} = \{\widehat{q}_1, \widehat{q}_2, \ldots, \widehat{q}_N\}^{\mathrm{T}} \tag{28}$$

and

$$\widehat{\boldsymbol{\varphi}} = \{\widehat{\varphi}_1, \widehat{\varphi}_2, \ldots, \widehat{\varphi}_N\} \tag{29}$$

Substitution of Eq. (27) into Eq. (3) yields the following:

$$\sum_{n=1}^{N} \left\{ \widehat{\varphi}_n''''\widehat{q}_n + \sum_{i=1}^{J} c_i \widehat{\varphi}_n \delta(\tilde{x}-\alpha_i) \frac{\partial \widehat{q}_n}{\partial \tilde{t}} + \widehat{\varphi}_n \frac{\partial^2 \widehat{q}_n}{\partial \tilde{t}^2} \right\} = \tilde{f}(\tilde{x},\tilde{t}) \tag{30}$$

Integration of Eq. (30) that is premultiplied by $\widehat{\varphi}_k$ results in

$$\sum_{n=1}^{N} \left\{ \left[\int_0^1 \widehat{\varphi}_k'' \widehat{\varphi}''_n \mathrm{d}\tilde{x} \right] \widehat{q}_n + \left[\sum_{i=1}^{J} c_i \widehat{\varphi}_k(\alpha_i)\,\widehat{\varphi}_n(\alpha_i) \right] \frac{\partial \widehat{q}_n}{\partial \tilde{t}} + \left[\int_0^1 \widehat{\varphi}_k \widehat{\varphi}_n \mathrm{d}\tilde{x} \right] \frac{\partial^2 \widehat{q}_n}{\partial \tilde{t}^2} \right\} = \int_0^1 \widehat{\varphi}_k \tilde{f} \mathrm{d}\tilde{x} \tag{31}$$

Because Eq. (31) holds for all $\widehat{\varphi}_k$, $k = 1, 2, \ldots, N$, Eq. (31) yields a modal reduced system, i.e.,

$$\widehat{\boldsymbol{M}} \frac{\mathrm{d}^2 \widehat{\boldsymbol{q}}}{\mathrm{d}\tilde{t}^2} + \widehat{\boldsymbol{C}} \frac{\mathrm{d}\widehat{\boldsymbol{q}}}{\mathrm{d}\tilde{t}} + \widehat{\boldsymbol{K}}\widehat{\boldsymbol{q}} = \widehat{\boldsymbol{F}} \tag{32}$$

where $\widehat{\boldsymbol{M}}$, $\widehat{\boldsymbol{C}}$, and $\widehat{\boldsymbol{K}}$ are the mass, damping, and stiffness matrices of the system in a modal space, respectively; $\widehat{\boldsymbol{F}}$ is the force vector in the modal space. By taking advantage of the orthogonality conditions of Eq. (26), the matrices can be computed as follows:

$$\widehat{\boldsymbol{M}} = \mathrm{diag}(\widehat{M}_{kk}) \quad k = 1, 2, \ldots, N; \ \widehat{M}_{kk} = \int_0^1 \widehat{\varphi}_k \widehat{\varphi}_k \mathrm{d}\tilde{x} \tag{33}$$

$$\widehat{\boldsymbol{C}} = [\widehat{C}_{kn}] \quad k = 1, 2, \ldots, N; \ n = 1, 2, \ldots, N$$
$$\widehat{C}_{kn} = \sum_{i=1}^{J} c_i \widehat{\varphi}_k(\alpha_i)\,\widehat{\varphi}_n(\alpha_i) \tag{34}$$

$$\widehat{\boldsymbol{K}} = \mathrm{diag}(\widehat{K}_{kk}) \quad k = 1, 2, \ldots, N; \ \widehat{K}_{kk} = \widehat{\omega}_k^2 \widehat{M}_{kk} \tag{35}$$

$$\widehat{\boldsymbol{F}} = \{\widehat{F}_1, \widehat{F}_2, \ldots, \widehat{F}_k, \ldots, \widehat{F}_N\}^{\mathrm{T}} \tag{36}$$
$$k = 1, 2, \ldots, N; \ \widehat{F}_k = \int_0^1 \widehat{\varphi}_k \tilde{f} \mathrm{d}\tilde{x}$$

The damping matrix in which not all off-diagonal terms are zero implies that this system is NCDS. Accordingly, the eigenvalues and eigenfunctions obtained by Eq. (32) have complex values, and the natural frequencies obtained by Eq. (32) are approximations of those of the original system. Furthermore, the eigenfunctions of the original system can be approximately computed by

$$\boldsymbol{\psi} \approx \widehat{\boldsymbol{\varphi}}\widehat{\boldsymbol{\chi}}, \quad \widehat{\boldsymbol{\chi}} = [\widehat{\boldsymbol{\eta}}_1 \quad \widehat{\boldsymbol{\eta}}_2 \quad \cdots \quad \widehat{\boldsymbol{\eta}}_k \quad \cdots \quad \widehat{\boldsymbol{\eta}}_{2N}] \tag{37}$$

where $\widehat{\boldsymbol{\chi}}$ is an $N \times 2N$ complex-valued modal matrix and $\widehat{\boldsymbol{\eta}}_k$ is the k-th complex mode vector of the reduced system.

3 Methodologies for Dynamic Response

The formulations for the responses in the time and frequency domains based on the CMS and AM methods are presented in this section. Furthermore, the formulas for the variance analysis are provided.

We assume that the external excitation is separable, i.e., in the following form:

$$\tilde{f}(\tilde{x},\tilde{t}) = \tilde{w}(\tilde{x})\,\tilde{v}(\tilde{t}) \tag{38}$$

where $\tilde{w}(\tilde{x})$ is the shape function and $\tilde{v}(\tilde{t})$ is the time-varying load.

The motion equations for both the CMS and AM methods can be generally formed in the state space as follows:

$$\frac{\mathrm{d}}{\mathrm{d}\tilde{t}}\tilde{z}_s = \boldsymbol{A}_s \tilde{z}_s + \boldsymbol{B}_s \tilde{v}(\tilde{t}) \tag{39a}$$

$$\tilde{\boldsymbol{y}}_s = \boldsymbol{C}_s \tilde{z}_s \tag{39b}$$

Thus, for the CMS method, the matrices in Eq. (39) are

$$\tilde{z}_s = \boldsymbol{q}, \ \boldsymbol{A}_s = \boldsymbol{\Omega}, \ \boldsymbol{B}_s = \boldsymbol{B}\boldsymbol{B}_{\mathrm{F}}$$
$$\boldsymbol{B}_{\mathrm{F}} = \left\{ \int_0^1 \psi_1 \tilde{w} \mathrm{d}\tilde{x}, \int_0^1 \psi_2 \tilde{w} \mathrm{d}\tilde{x}, \ldots, \int_0^1 \psi_{2N} \tilde{w} \mathrm{d}\tilde{x} \right\}^{\mathrm{T}}, \ \boldsymbol{C}_s = \boldsymbol{I} \tag{40}$$

where $\boldsymbol{I}$ is an identity matrix. For the AM method, the matrices in Eq. (39) are

$$\tilde{z}_s = \begin{Bmatrix} \widehat{\boldsymbol{q}} \\ \dfrac{\mathrm{d}}{\mathrm{d}\tilde{t}}\widehat{\boldsymbol{q}} \end{Bmatrix},\ \boldsymbol{A}_s = \begin{bmatrix} \boldsymbol{0} & \boldsymbol{I} \\ -\widehat{\boldsymbol{M}}^{-1}\widehat{\boldsymbol{K}} & -\widehat{\boldsymbol{M}}^{-1}\widehat{\boldsymbol{C}} \end{bmatrix},\ \boldsymbol{B}_s = \begin{bmatrix} \boldsymbol{0} \\ \widehat{\boldsymbol{M}}^{-1}\widehat{\boldsymbol{B}}_F \end{bmatrix}$$

$$\widehat{\boldsymbol{B}}_F = \left\{ \int_0^1 \widehat{\varphi}_1 \tilde{w}\mathrm{d}\tilde{x}, \int_0^1 \widehat{\varphi}_2 \tilde{w}\mathrm{d}\tilde{x}, \ldots, \int_0^1 \widehat{\varphi}_N \tilde{w}\mathrm{d}\tilde{x} \right\}^{\mathrm{T}},\ \boldsymbol{C}_s = [\boldsymbol{I} \quad \boldsymbol{0}] \tag{41}$$

3.1 Time-domain analysis

In the CMS method, the initial conditions of the system satisfy the following requirement:

$$\begin{Bmatrix} \tilde{y}(x,0) \\ \dfrac{\partial}{\partial\tilde{t}}\tilde{y}(x,0) \end{Bmatrix} = \begin{bmatrix} \boldsymbol{\psi} \\ \boldsymbol{\Lambda}^{\circ}\boldsymbol{\psi} \end{bmatrix} \boldsymbol{q}(0) \tag{42}$$

where $\boldsymbol{q}(0)$ is the corresponding initial condition in the modal state space. Integration of Eq. (42) premultiplied by $[\boldsymbol{\psi}^{\mathrm{T}} \quad (\boldsymbol{\Lambda}^{\circ}\boldsymbol{\psi})^{\mathrm{T}}]$ leads to

$$\boldsymbol{q}(0) = \frac{\displaystyle\int_0^1 [\boldsymbol{\psi}^{\mathrm{T}} \quad (\boldsymbol{\Lambda}^{\circ}\boldsymbol{\psi})^{\mathrm{T}}] \begin{Bmatrix} \tilde{y}(x,0) \\ \dfrac{\partial}{\partial\tilde{t}}\tilde{y}(x,0) \end{Bmatrix} \mathrm{d}\tilde{x}}{\displaystyle\int_0^1 [\boldsymbol{\psi}^{\mathrm{T}} \quad (\boldsymbol{\Lambda}^{\circ}\boldsymbol{\psi})^{\mathrm{T}}] \begin{bmatrix} \boldsymbol{\psi} \\ \boldsymbol{\Lambda}^{\circ}\boldsymbol{\psi} \end{bmatrix} \mathrm{d}\tilde{x}} \tag{43}$$

Thus, the vibration in the modal space induced by the initial condition can be expressed as

$$\boldsymbol{q} = \exp(\boldsymbol{\Omega})\boldsymbol{q}(0) \tag{44}$$

In the AM method, the initial conditions of the system satisfy the following:

$$\tilde{y}(\tilde{x},0) = \widehat{\boldsymbol{\varphi}}\widehat{\boldsymbol{q}}(0) \tag{45}$$

where $\widehat{\boldsymbol{q}}(0)$ is the corresponding initial condition in the AM-method-based modal space. Integration of Eq. (45) premultiplied by $\widehat{\boldsymbol{\varphi}}^{\mathrm{T}}$ results in

$$\widehat{\boldsymbol{q}}(0) = \frac{\displaystyle\int_0^1 \widehat{\boldsymbol{\varphi}}^{\mathrm{T}}\tilde{y}(\tilde{x},0)\,\mathrm{d}\tilde{x}}{\displaystyle\int_0^1 \widehat{\boldsymbol{\varphi}}^{\mathrm{T}}\widehat{\boldsymbol{\varphi}}\mathrm{d}\tilde{x}} \tag{46}$$

In a similar manner, we can obtain

$$\frac{\mathrm{d}}{\mathrm{d}\tilde{t}}\widehat{\boldsymbol{q}}(0) = \frac{\displaystyle\int_0^1 \widehat{\boldsymbol{\varphi}}^{\mathrm{T}} \frac{\partial}{\partial\tilde{t}}\tilde{y}(\tilde{x},0)\,\mathrm{d}\tilde{x}}{\displaystyle\int_0^1 \widehat{\boldsymbol{\varphi}}^{\mathrm{T}}\widehat{\boldsymbol{\varphi}}\mathrm{d}\tilde{x}} \tag{47}$$

Eq. (41) shows that the reduced-order system in a modal space obtained via the AM method is described by real-valued matrices. Hence, the response of the system subjected to external excitation can be obtained via conventional means. In comparison, obtaining the response of the reduced-order system derived via the CMS method is more difficult because of the presence of complex-valued matrices. The following presents a transformation technique whereby the motion equation with complex-valued matrices can be transformed into one equation with real-valued matrices.

Eq. (39a) can be reformulated as follows:

$$\frac{\mathrm{d}}{\mathrm{d}\tilde{t}}[\mathrm{Re}(\tilde{z}_s) + \mathrm{j}\mathrm{Im}(\tilde{z}_s)] = [\mathrm{Re}(\boldsymbol{A}_s) + \mathrm{j}\mathrm{Im}(\boldsymbol{A}_s)][\mathrm{Re}(\tilde{z}_s) + \mathrm{j}\mathrm{Im}(\tilde{z}_s)] + [\mathrm{Re}(\boldsymbol{B}_s) + \mathrm{j}\mathrm{Im}(\boldsymbol{B}_s)]\tilde{v}(\tilde{t}) \tag{48}$$

Rewriting Eq. (48) in a state-space form yields

$$\frac{\mathrm{d}}{\mathrm{d}\tilde{t}}\begin{bmatrix} \mathrm{Re}(\tilde{z}_s) \\ \mathrm{Im}(\tilde{z}_s) \end{bmatrix} = \begin{bmatrix} \mathrm{Re}(\mathrm{A}_s) & -\mathrm{Im}(\boldsymbol{A}_s) \\ \mathrm{Im}(\boldsymbol{A}_s) & \mathrm{Re}(\boldsymbol{A}_s) \end{bmatrix}\begin{bmatrix} \mathrm{Re}(\tilde{z}_s) \\ \mathrm{Im}(\tilde{z}_s) \end{bmatrix} + \begin{bmatrix} \mathrm{Re}(\boldsymbol{B}_s) \\ \mathrm{Im}(\boldsymbol{B}_s) \end{bmatrix}\tilde{v}(\tilde{t}) \tag{49}$$

As the matrices in Eq. (49) have real values, Eq. (49) can now be easily solved. Accordingly, the output governed by Eq. (39b) is expressed as

$$\tilde{\boldsymbol{y}}_s = [\boldsymbol{C}_s \quad \mathrm{j}\boldsymbol{C}_s]\begin{bmatrix} \mathrm{Re}(\tilde{z}_s) \\ \mathrm{Im}(\tilde{z}_s) \end{bmatrix} \tag{50}$$

3.2 Transfer function

As the system is linear, the multiple-input-multiple-output (MIMO) response can be regarded as the sum of a series of single-input-single-output (SISO) responses. Thus, the methodologies presented in the following for a SISO problem can be easily extended to that for a MIMO problem.

Let us consider a SISO problem in which the input is a concentrated excitation located at $\tilde{x} = \beta$ and the output is the response at point $\tilde{x} = \tilde{x}_{\mathrm{out}}$. Corresponding transfer function $H(S)$ obtained by the CMS method is then expressed as

$$H(S) = \sum_{n=1}^{2N} \psi_n(\tilde{x}_{\mathrm{out}}) H_n^{\mathrm{modal}}(S) \tag{51}$$

where S is a nondimensional frequency; $H_n^{\mathrm{modal}}(S)$ is the transfer function in the complex modal space. $H_n^{\mathrm{modal}}(S)$ can be obtained by

$$H_n^{\mathrm{modal}}(S) = \frac{L(q_n(\tilde{t}))}{L(\tilde{v}(\tilde{t}))} \tag{52}$$

where $L(\ )$ indicates the operation of Laplace transformation. In a similar manner, transfer function $\widehat{H}_n^{\mathrm{modal}}(S)$ based on the AM method can be obtained as

$$\widehat{H}(S) = \sum_{n=1}^{N} \widehat{\varphi}_n(\tilde{x}_{\mathrm{out}}) \widehat{H}_n^{\mathrm{modal}}(S) \tag{53}$$

where $\widehat{H}_n^{\mathrm{modal}}(S)$ is the transfer function in the AM-based modal space, which is given as

$$\widehat{H}_n^{\text{modal}}(S) = \frac{L(\widehat{q}_n(\tilde{t}))}{L(\tilde{v}(\tilde{t}))} \tag{54}$$

The transfer functions can be easily obtained by applying Laplace transformation to Eqs. (39) to (41). For a SISO problem, the shape function of the excitation in Eqs. (40) and (41) is

$$\tilde{w}(\tilde{x}) = \delta(\tilde{x} - \beta) \tag{55}$$

We note that the nondimensional concentrated load shown in Eq. (55) corresponds to a dimensional concentrated load, i. e., $w(x) = ml^2\omega_0^2\delta(x - \beta l)$. Furthermore, matrix $\boldsymbol{B}_{\text{F}}$ in Eq. (40) is

$$\boldsymbol{B}_{\text{F}} = \{\psi_1(\beta), \psi_2(\beta), \ldots, \psi_{2N}(\beta)\}^{\text{T}} \tag{56}$$

and matrix $\widehat{\boldsymbol{B}}_{\text{F}}$ in Eq. (41) is

$$\widehat{\boldsymbol{B}}_{\text{F}} = \{\widehat{\varphi}_1(\beta), \widehat{\varphi}_2(\beta), \ldots, \widehat{\varphi}_N(\beta)\}^{\text{T}} \tag{57}$$

3.3 Variance

Provided that an external force is in a separable form of Eq. (38) and its time-varying part $\tilde{v}(\tilde{t})$ is a white noise with a noise intensity of W, the covariance matrix of the system is then expressed as

$$E(\tilde{\boldsymbol{y}}_{\text{s}}\overline{\tilde{\boldsymbol{y}}_{\text{s}}}^{\text{T}}) = \boldsymbol{C}_{\text{s}}\boldsymbol{Q}_{\text{s}}\boldsymbol{C}_{\text{s}}^{\text{T}} \tag{58}$$

where $\boldsymbol{Q}$ can be obtained by solving the Lyapunov equation

$$\boldsymbol{A}_{\text{s}}\boldsymbol{Q}_{\text{s}} + \boldsymbol{Q}_{\text{s}}\overline{\boldsymbol{A}_{\text{s}}}^{\text{T}} + \boldsymbol{B}_{\text{s}}W\overline{\boldsymbol{B}_{\text{s}}}^{\text{T}} = 0 \tag{59}$$

Thus, in the CMS method, the variance in the output can be computed using the following:

$$E\{\tilde{y}(\tilde{x}_{\text{out}}, t)\,\tilde{y}(\tilde{x}_{\text{out}}, \tilde{t})\} = E\{\boldsymbol{\psi}(\tilde{x}_{\text{out}})\tilde{\boldsymbol{y}}_{\text{s}}(\overline{\boldsymbol{\psi}(\tilde{x}_{\text{out}})\tilde{\boldsymbol{y}}_{\text{s}}})^{\text{T}}\} = \text{trace}\{\overline{\boldsymbol{\psi}(\tilde{x}_{\text{out}})}^{\text{T}}\boldsymbol{\psi}(\tilde{x}_{\text{out}})\,E(\tilde{\boldsymbol{y}}_{\text{s}}\overline{\tilde{\boldsymbol{y}}_{\text{s}}}^{\text{T}})\} \tag{60}$$

For the average of the variance response of the entire beam, namely, spatial average variance, we can obtain

$$E\left\{\int_0^1 \tilde{y}(\tilde{x}, t)\,\tilde{y}(\tilde{x}, t)\,\mathrm{d}\tilde{x}\right\} = E\left\{\int_0^1 \boldsymbol{\psi}\tilde{\boldsymbol{y}}_s(\overline{\boldsymbol{\psi}\tilde{\boldsymbol{y}}_s})^{\text{T}}\mathrm{d}\tilde{x}\right\} = \text{trace}\left\{\left(\int_0^1 \overline{\boldsymbol{\psi}}^{\text{T}}\boldsymbol{\psi}\mathrm{d}x\right)E(\tilde{\boldsymbol{y}}_{\text{s}}\overline{\tilde{\boldsymbol{y}}_{\text{s}}}^{\text{T}})\right\} \tag{61}$$

When the AM method is used, $\widehat{\boldsymbol{\varphi}}$ can be substituted for $\boldsymbol{\psi}$ in Eqs. (60) and (61).

Eqs. (60) and (61), in which white noise is considered as an external excitation, can be easily applied to variance estimation of many stationary random processes, which can be regarded as filtered white noise. Subsequently, we introduce an example in which the random excitation is a band-limited white noise (BLWN).

BLWN can be regarded as white noise filtered by a band-pass filter in the following form:

$$\frac{\mathrm{d}}{\mathrm{d}\tilde{t}}\tilde{\boldsymbol{u}}_{\text{f}} = \boldsymbol{A}_{\text{f}}\tilde{\boldsymbol{u}}_{\text{f}} + \boldsymbol{B}_{\text{f}}\tilde{v}_{\text{f}}(\tilde{t}) \tag{62a}$$

$$\tilde{\boldsymbol{y}}_{\text{f}} = \boldsymbol{C}_{\text{f}}\tilde{\boldsymbol{u}}_{\text{f}} \tag{62b}$$

where $\boldsymbol{A}_{\text{f}}$, $\boldsymbol{B}_{\text{f}}$, and $\boldsymbol{C}_{\text{f}}$ are the state, input, and output matrices, respectively; $\tilde{\boldsymbol{u}}_{\text{f}}$ is the state vector of the filter; $\tilde{v}_{\text{f}}(\tilde{t})$ is the white noise with noise intensity W to be filtered; $\tilde{y}_{\text{f}}$ is the output vector of the filter. Thus, $\tilde{v} = \tilde{y}_{\text{f}}$.

The combination of Eqs. (62) and (39) leads to an augmented system, i. e.,

$$\frac{\mathrm{d}}{\mathrm{d}\tilde{t}}\tilde{z}_{\text{a}} = \boldsymbol{A}_{\text{a}}\tilde{z}_{\text{a}} + \boldsymbol{B}_{\text{a}}\tilde{v}_{\text{f}}(\tilde{t}) \tag{63a}$$

$$\tilde{\boldsymbol{y}}_{\text{s}} = \boldsymbol{C}_{\text{a}}\tilde{z}_{\text{a}} \tag{63b}$$

where

$$\tilde{z}_{\text{a}} = \begin{Bmatrix}\tilde{z}_{\text{s}}\\ \tilde{\boldsymbol{u}}_{\text{f}}\end{Bmatrix},\ \boldsymbol{A}_{\text{a}} = \begin{bmatrix}\boldsymbol{A}_{\text{s}} & \boldsymbol{B}_{\text{s}}\boldsymbol{C}_{\text{f}}\\ \boldsymbol{0} & \boldsymbol{A}_{\text{f}}\end{bmatrix},\ \boldsymbol{B}_{\text{a}} = \begin{Bmatrix}\boldsymbol{0}\\ \boldsymbol{B}_{\text{f}}\end{Bmatrix},\ \boldsymbol{C}_{\text{a}} = [\boldsymbol{C}_{\text{s}}\quad \boldsymbol{0}] \tag{64}$$

Thus, the covariance matrix of the beam-damper system herein subjected to BLWN is

$$E(\tilde{\boldsymbol{y}}_{\text{s}}\overline{\tilde{\boldsymbol{y}}_{\text{s}}}^{\text{T}}) = \boldsymbol{C}_{\text{a}}\boldsymbol{Q}_{\text{a}}\boldsymbol{C}_{\text{a}}^{\text{T}} \tag{65}$$

where $\boldsymbol{Q}_{\text{a}}$ is the solution of the Lyapunov equation, i. e.,

$$\boldsymbol{A}_{\text{a}}\boldsymbol{Q}_{\text{a}} + \boldsymbol{Q}_{\text{a}}\overline{\boldsymbol{A}_{\text{a}}}^{\text{T}} + \boldsymbol{B}_{\text{a}}W\overline{\boldsymbol{B}_{a}}^{\text{T}} = \boldsymbol{0} \tag{66}$$

Thus, the BLWN-induced response can be easily obtained by substituting Eq. (65) into Eqs. (60) and (61).

4 Numerical Study on the Dynamic Response

FEA is employed in this study to validate the proposed theoretical approach. The element utilized in FEA is an ordinary in-plane beam element. Thus, in FEA, the motion equation of the beam with attached dampers is formulated as

$$\boldsymbol{M}\frac{\mathrm{d}^2}{\mathrm{d}t^2}\boldsymbol{y}(t) + \boldsymbol{C}\frac{\mathrm{d}}{\mathrm{d}t}\boldsymbol{y}(t) + \boldsymbol{K}\boldsymbol{y}(t) = \boldsymbol{F}(t) \tag{67}$$

where $\boldsymbol{M}$, $\boldsymbol{C}$, and $\boldsymbol{K}$ are the mass, damping, and stiffness matrices, respectively; $\boldsymbol{F}$ is the vector of the external nodal excitations; $\boldsymbol{y}$ is the vector of the nodal displacements. The function of the dampers is introduced by revising dimensional damping matrix $\boldsymbol{C}$ according to the relationship between the dimensional and nondimensional damping expressed in Eq. (2).

Furthermore, Eq. (67) yields the following relationship using nondimensional $\tilde{t}$ and the nondimensional external load expressed in Eqs. (2) and (4), respectively:

$$\omega_0^2\boldsymbol{M}\frac{\mathrm{d}^2}{\mathrm{d}\tilde{t}^2}\tilde{\boldsymbol{y}}(\tilde{t}) + \omega_0\boldsymbol{C}\frac{\mathrm{d}}{\mathrm{d}\tilde{t}}\tilde{\boldsymbol{y}}(\tilde{t}) + \boldsymbol{K}\tilde{\boldsymbol{y}}(\tilde{t}) = ml\omega_0^2\tilde{\boldsymbol{F}}(\tilde{t}) \tag{68}$$

where $\tilde{\boldsymbol{y}}(\tilde{t})$ is the nondimensional displacement vector and

$\tilde{\boldsymbol{F}}(\tilde{t})$ is the nondimensional force vector. The i-th entry of $\tilde{\boldsymbol{F}}(\tilde{t})$ can be computed by $\tilde{F}_i(\tilde{t}) = \dfrac{1}{ml^2\omega_0^2}F_i(t) = \int_{\tilde{L}_i} \tilde{w}(\tilde{x}, \tilde{t})\,\mathrm{d}\tilde{x}$, where $F_i(t)$ is the i-th entry of F, and $\tilde{L}_i$ is the ratio of the length of the i-th element to that of the entire beam.

Nondimensional static deflection $\tilde{y}(\tilde{x})$ due to static concentrated forces can be obtained by solving the following:

$$\frac{\mathrm{d}^4}{\mathrm{d}\tilde{x}^4}\tilde{y}(\tilde{x}) = \sum_{i=1}^{J} \tilde{f}_i \delta(\tilde{x} - \tilde{\gamma}_i) \tag{69}$$

where J is the number of concentrated forces; $\tilde{f}_i$ and $\tilde{\gamma}_i$ are the size and location of the i-th external static concentrated force, respectively. Thus, the theoretical solution of $\tilde{y}(\tilde{x})$ can be expressed as

$$\tilde{y}(\tilde{x}) = \frac{1}{6}\sum_{i=1}^{J} \tilde{f}_i \{H(\tilde{x} - \tilde{\gamma}_i)(\tilde{x} - \tilde{\gamma}_i)^3 - \tilde{x}^2(\tilde{x} - 3\tilde{\gamma}_i)\} \tag{70}$$

We consider an example where two identical dampers are employed, which are located at $\tilde{x} = 0.2$ and $\tilde{x} = 0.8$, i.e., $\alpha_1 = 0.2$ and $\alpha_2 = 0.8$, respectively, as shown in Fig. 2. This arrangement is also used in the other cases in this study. The theoretical static deformation of a cantilever beam subjected to a unit concentrated force at its midpoint is compared with the numerical results obtained using Eq. (68), as shown in Fig. 2. The results by FEA are found to very well match the exact results of Eq. (70). We note that the stiffness produced by the dampers in terms of static response is zero.

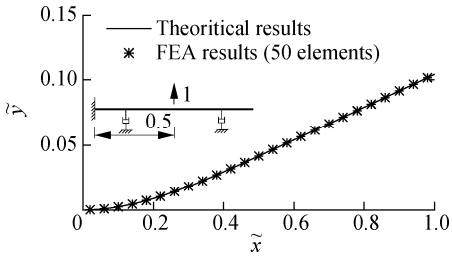

Fig. 2 Static deformations caused by a unit concentrated force at the midpoint

The static deformation shown in Fig. 2 is set as the initial condition of the system. For the corresponding free vibration caused by the static deformation of the system shown in Fig. 2, the time histories of the selected points are shown in Fig. 3. The CMS results shown in the figure are those obtained by Eq. (44), and the FEA and AM results are those computed using the "lsim" function of MATLAB. The curves obtained by FEA and the CMS and AM methods are found to be very close, which validates all these three methods. Note that no overdamped mode is found in the case of small damping with a value of $c = 1.0$. The existence of overdamped modes in the large damping case ($c = 50.0$) slows down the process of approaching the original equilibrium position from the initial disturbance.

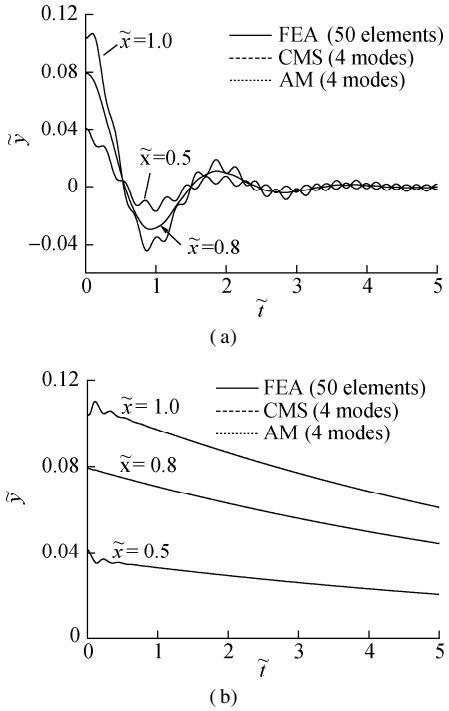

Fig. 3 Time histories of the free vibration due to initial disturbance. (a) $c = 1.0$; (b) $c = 50.0$

Fig. 4 shows the variance in the tip-displacement response and spatial average variance, which varies with the strength of the damper, with respect to the system shown in Fig. 2. A concentrated force and a uniformly

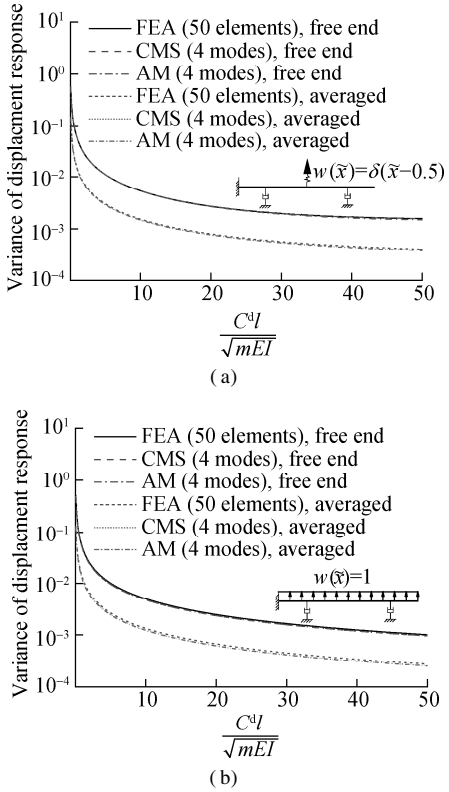

Fig. 4 Variance response induced by external forces. (a) Concentrated force; (b) Uniformly distributed force

distributed force, which varies with time in accordance with a white noise with a noise intensity value of unity, are individually employed to excite beam vibration. We can observe that in terms of the variance response, the results obtained by the FEA, CMS, and AM methods are rather close. The curves of the variance in the free-end response exhibit a trend similar to those of the spatial average variance, although the former is naturally higher than the latter. Generally, as shown in Fig. 4, the monotonically decreasing variance responses indicate that higher damping of the dampers can result in a smaller dynamic response. However, the efficiency of suppressing the vibration by increasing the damping decreases with increasing damping.

Fig. 5 shows the transfer functions of a SISO system in which the damped beam shown in Fig. 2 is considered. The input is a concentrated force at the midpoint of the beam, and the output is the displacement response of the free end. At small damping, the transfer functions obtained by the three methods are almost identical. However, when the damping is large, the transfer functions realized by the CMS method remain close to those obtained by FEA. However, the AM-method-based results show a large difference, implying that the CMS method performs better than the AM method in the frequency-domain analysis.

In the time domain, we find that the CMS method also provides a more accurate result than the AM method, especially when large damping results in the appearance of overdamped modes. Fig. 6 shows the time histories of the tip vibration in the case of large and small damping, which considers the damped beam shown in Fig. 2. A sinusoidal excitation with an amplitude of unity is applied to the midpoint in which the circular frequency of the excitation is equal to the imaginary part of the natural frequency that corresponds to the second mode. We find that the results of the three methods are very close in the case of small damping. However, in the case of large damping, the peak values of the curve obtained by the AM method are obviously smaller than those obtained by FEA. Meanwhile, the results based on the CMS method agree well with the FEA results.

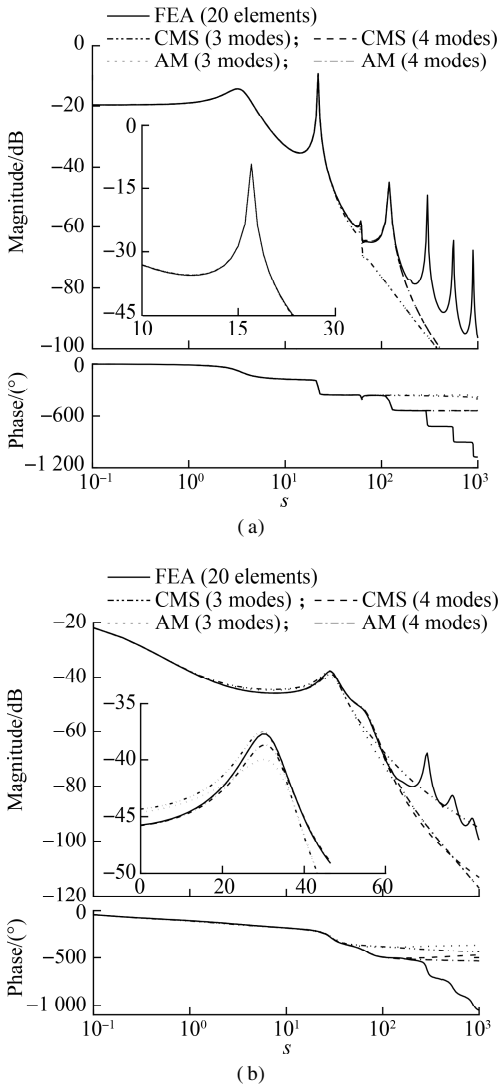

Fig. 5 Selected transfer functions. (a) $c = 1.0$; (b) $c = 50.0$

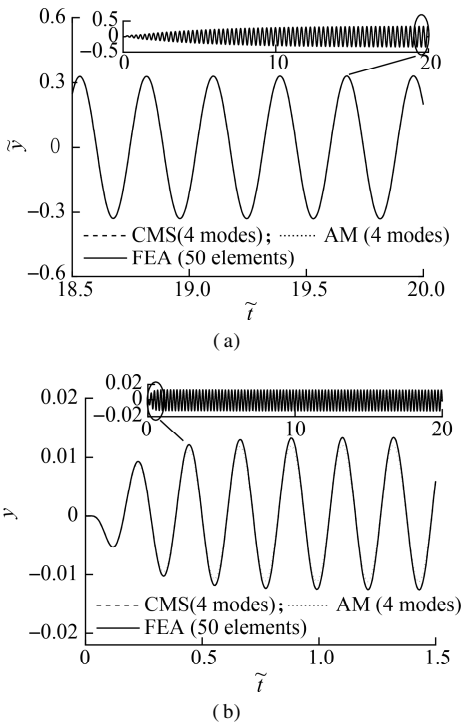

Fig. 6 Time histories of the free end. (a) $c = 1.0$; (b) $c = 50.0$

A random vibration analysis is performed using a random excitation in the form of BLWN to further show the effectiveness of the CMS method. BLWN is generated by filtering a white noise with unit noise intensity. The nondimensional central frequency of BLWN is 27.5, and the bandwidth is 15; thus, the natural frequency corresponding to the second mode is covered. The filter is a Butterworth band-pass filter. The variance responses of the free end are shown in Fig. 7, in which the employed system is the same as the damped beam shown in Fig. 2. Once

again, in the case of small damping, the results from the CMS, AM, and FE methods are very close, while in the case of large damping, the curves resulting from the FEA and AM methods are inconsistent. The divergence becomes more significant as the damping increases. In contrast, the difference between the results via the CMS method and FEA remains very small, which again highlights the superiority of the CMS method.

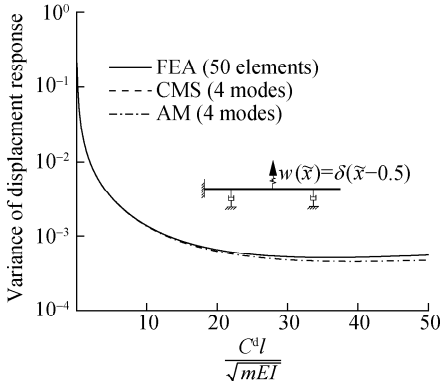

Fig. 7 Variance of the displacement response of the free end

5 Optimal Damping and Locations under Random Excitation

The optimal locations and optimal damping of the dampers have been recognized to strongly depend on what types of optimization objective and external excitation are considered. For illustrative purposes, the optimization problem herein is related to a cantilevered beam with two attached identical dampers. The beam is subjected to a concentrated time-varying random force, which is a white noise with unit noise intensity. The enumeration technique is employed to perform this study in which the increments of the damping and damper location are 0.10 and 0.02, respectively. In other words, all the combinations of the nondimensional damping coefficients and locations of the dampers are investigated.

With regard to the variance response of the free end, the optimal installation that minimizes the variance is that the two dampers should be identically installed at the free end. For a spatial average variance, the variations of the least average variances from the nondimensional damping are shown in Fig. 8(a), and the corresponding optimal locations are shown in Fig. 8(b). The case of $\alpha_1 = \alpha_2$ indicates that two identical dampers are installed at the same location, which is equivalent to the case of using a single damper but with double damping. The curves resulting from the CMS and AM methods are fairly close. We find that in the case of small damping ($c \leqslant 2.4$), no large difference exists between the strategies of using one large damper and using two small dampers; these two strategies yield almost the same optimal location and effectiveness in vibration control. When $c \leqslant 2.4$, installing the dampers at the free end produces a minimum average variance. When $c \geqslant 2.4$, installing two dampers at distinct locations is better than installing them at the same location, i.e., the use of two small dampers demonstrates better performance than the use of one large damper for vibration suppression. Moreover, as shown in Fig. 8, the least average variance decreases with the increase in damping, provided that the optimal damping and optimal damping location are considered.

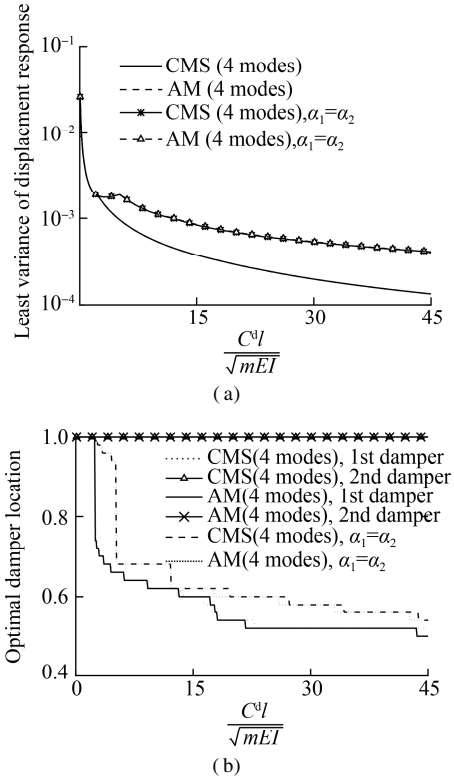

Fig. 8 Optimization problem. (a) Least variance; (b) Optimal location

6 Conclusions

1) Compared with the AM method, the CMS method can better reflect the inherent complex dynamic characteristics in NCDSs and results in a reduced-order model with higher accuracy, provided that the same number of modes are considered for orthogonal decomposition of forced vibration. Nevertheless, once the overdamped modes, which are not complex conjugate, are involved, the conventional CMS theory for NCDS needs to be further modified. An ICMS theory is proposed in this study where the underdamped complex modes are complex conjugates, and a pair of overdamped complex modes consist of the modes that correspond to two real-valued solutions of the same characteristic equation.

2) Methodologies associated with the AM and CMS methods are presented in detail for the time-domain, frequency-domain, and variance analyses to facilitate the forced vibration analysis of NCDSs. With reference to the time-domain analysis, the original complex-valued state-space equation is transformed into an augmented real-val-

ued state-space equation by splitting the original matrices into real and imaginary parts and reassembling the equation so that many existing methods for time-history analysis can be utilized. With regard to the response induced by the filtered white-noise excitation, a Lyapunov equation-based variance analysis method is proposed, which is capable of rapid computation.

3) A cantilevered beam with two attached identical external dampers is used for the numerical case study. The results from the ICMS method are compared with those from the AM method and FEA. We find that the results from the CMS method are closer to those from FEA, which highlights the superiority of the CMS method over the AM method in dealing with NCDSs. The study of optimal damping and optimal damper location using the enumeration method shows that given small damping of the damper(s), no difference is observed between the use of a single damper and multiple dampers; however, the latter performs better provided that the damping of the dampers is relatively large.

References

[1] Main J A, Krenk S. Efficiency and tuning of viscous dampers on discrete systems[J]. *Journal of Sound and Vibration*, 2005, **286**(1/2): 97 − 122. DOI: 10.1016/j.jsv.2004.09.022.

[2] Caughey T K, O'Kelly M E J. Classical normal modes in damped linear dynamic systems[J]. *Journal of Applied Mechanics*, 1965, **32**(3): 583 − 588. DOI: 10.1115/1.3627262.

[3] Srikantha P A. On the necessary and sufficient conditions for the existence of classical normal modes in damped linear dynamic systems[J]. *Journal of Sound and Vibration*, 2003, **264**(3): 741 − 745. DOI: 10.1016/S0022-460X(02)01506-7.

[4] Hassanpour P A, Esmailzadeh E, Cleghorn W L, et al. Generalized orthogonality condition for beams with intermediate lumped masses subjected to axial force[J]. *Journal of Vibration and Control*, 2010, **16**(5): 665 − 683. DOI: 10.1177/1077546309106526.

[5] Warburton G B. Soil-structure interaction for tower structures[J]. *Earthquake Engineering & Structural Dynamics*, 1978, **6**(6): 535 − 556. DOI: 10.1002/eqe.4290060603.

[6] Wu J S, Lin T L. Free vibration analysis of a uniform cantilever beam with point masses by an analytical-and-numerical-combined method[J]. *Journal of Sound and Vibration*, 1990, **136**(2): 201 − 213. DOI: 10.1016/0022-460X(90)90851-P.

[7] Pacheco B M, Fujino Y, Sulekh A. Estimation curve for modal damping in stay cables with viscous damper[J]. *Journal of Structural Engineering*, 1993, **119**(6): 1961 − 1979. DOI: 10.1061/(asce)0733-9445(1993)119: 6(1961).

[8] Gürgöze M. On the eigenvalues of viscously damped beams, carrying heavy masses and restrained by linear and torsional springs[J]. *Journal of Sound and Vibration*, 1997, **208**(1): 153 − 158. DOI: 10.1006/jsvi.1997.1165.

[9] Wu J S, Chen D W. Dynamic analysis of a uniform cantilever beam carrying a number of elastically mounted point masses with dampers[J]. *Journal of Sound and Vibration*, 2000, **229**(3): 549 − 578. DOI: 10.1006/jsvi.1999.2504.

[10] Wu J J. Use of equivalent-damper method for free vibration analysis of a beam carrying multiple two degree-of-freedom spring-damper-mass systems[J]. *Journal of Sound and Vibration*, 2005, **281**(1/2): 275 − 293. DOI: 10.1016/j.jsv.2004.01.013.

[11] Chang T P. Forced vibration of a mass-loaded beam with a heavy tip body[J]. *Journal of Sound and Vibration*, 1993, **164**(3): 471 − 484. DOI: 10.1006/jsvi.1993.1229.

[12] Yang B. Exact receptances of nonproportionally damped dynamic systems[J]. *Journal of Vibration and Acoustics*, 1993, **115**(1): 47 − 52. DOI: 10.1115/1.2930313.

[13] Gürgöze M, Erol H. On the frequency response function of a damped cantilever simply supported in-span and carrying a tip mass[J]. *Journal of Sound and Vibration*, 2002, **255**(3): 489 − 500. DOI: 10.1006/jsvi.2001.4118.

[14] Gürgöze M, Erol H. Dynamic response of a viscously damped cantilever with a viscous end condition[J]. *Journal of Sound and Vibration*, 2006, **298**(1/2): 132 − 153. DOI: 10.1016/j.jsv.2006.04.042.

[15] Veletsos A S, Ventura C E. Modal analysis of non-classically damped linear systems[J]. *Earthquake Engineering & Structural Dynamics*, 1986, **14**(2): 217 − 243. DOI: 10.1002/eqe.4290140205.

[16] Foss K A. Co-ordinates which uncouple the equations of motion of damped linear dynamic systems[J]. *Journal of Applied Mechanics*, 1958, **25**(3): 361 − 364. DOI: 10.1115/1.4011828.

[17] Zhao Y P, Zhang Y M. Improved complex mode theory and truncation and acceleration of complex mode superposition[J]. *Advances in Mechanical Engineering*, 2016, **8**(10): 168781401667151. DOI: 10.1177/1687814016671510.

[18] de Domenico D, Ricciardi G. Dynamic response of non-classically damped structures via reduced-order complex modal analysis: Two novel truncation measures[J]. *Journal of Sound and Vibration*, 2019, **452**: 169 − 190. DOI: 10.1016/j.jsv.2019.04.010.

[19] Oliveto G, Santini A, Tripodi E. Complex modal analysis of a flexural vibrating beam with viscous end conditions[J]. *Journal of Sound and Vibration*, 1997, **200**(3): 327 − 345. DOI: 10.1006/jsvi.1996.0717.

[20] Oliveti G, Santini A. Complex modal analysis of a continuous model with radiation damping[J]. *Journal of Sound and Vibration*, 1996, **192**(1): 15 − 33. DOI: 10.1006/jsvi.1996.0173.

[21] Fan Z J, Lee J H, Kang K H, et al. The forced vibration of a beam with viscoelastic boundary supports[J]. *Journal of Sound and Vibration*, 1998, **210**(5): 673 − 682. DOI: 10.1006/jsvi.1997.1353.

[22] Krenk S. Complex modes and frequencies in damped structural vibrations[J]. *Journal of Sound and Vibration*, 2004, **270**(4/5): 981 − 996. DOI: 10.1016/S0022-460X(03)00768-5.

[23] Impollonia N, Ricciardi G, Saitta F. Dynamic behavior of stay cables with rotational dampers[J]. *Journal of Engineering Mechanics*, 2010, **136**(6): 697 - 709. DOI: 10.1061/(asce)em.1943-7889.0000115.
[24] Alati N, Failla G, Santini A. Complex modal analysis of rods with viscous damping devices[J]. *Journal of Sound and Vibration*, 2014, **333**(7): 2130 - 2163. DOI: 10.1016/j.jsv.2013.11.030.
[25] Chen Y, McFarland D M, Spencer B F Jr, et al. A beam with arbitrarily placed lateral dampers: Evolution of complex modes with damping[J]. *Journal of Vibration and Control*, 2018, **24**(2): 379 - 392. DOI: 10.1177/1077546316641592.
[26] Jacquot R G. Random vibration of damped modified beam systems[J]. *Journal of Sound and Vibration*, 2000, **234**(3): 441 - 454. DOI: 10.1006/jsvi.1999.2894.
[27] Jacquot R G. The spatial average mean square motion as an objective function for optimizing damping in damped modified systems[J]. *Journal of Sound and Vibration*, 2003, **259**(4): 955 - 965. DOI: 10.1006/jsvi.2002.5209.

考虑过阻尼模态参与的改进复模态叠加法

陈 勇[1,2] Donald M. McFarland[3,4] Billie F. Spencer, Jr.[2] Lawrence A. Bergman[3]

([1] 浙江大学建筑工程学院, 杭州 310027)
([2]Department of Civil and Environmental Engineering, University of Illinois at Urbana-Champaign, Urbana 61801, USA)
([3]Department of Aerospace Engineering, University of Illinois at Urbana-Champaign, Urbana 61801, USA)
([4] 浙江工业大学机械工程学院, 杭州 310014)

摘要:为处理非比例阻尼系统可能出现的过阻尼模态,提出了一种改进的复模态叠加强迫振动分析方法,建议无论模态是否过阻尼,复模态振动分析时应成对使用复模态. 以一个连接任意布置外部阻尼器的悬臂梁典型非比例阻尼系统为例,其第 1 阶模态会随阻尼系数的增加而过阻尼. 在厘清复模态响应与实际动力响应关系的基础上阐述了采用改进复模态叠加法获得时域响应、传递函数和方差的完整理论方法. 将方程分为实部和虚部,使得原复数域运动方程成为基于实数矩阵的增广状态空间方程,从而克服了采用复数矩阵计算时变响应的困难. 此外,针对基于白噪声滤波的外部激励,提出了一种高效方差响应评估方法,降低了计算资源消耗. 结果表明,相较于假设模态法,复模态叠加法的结果更接近于有限元结果. 基于遍历法研究最优阻尼器参数和位置时,采用多个小阻尼阻尼器优于单个大阻尼阻尼器.

关键词:非经典阻尼系统;连续系统;强迫振动;复模态叠加法;过阻尼模态;动力响应
中图分类号:TU311.3